Experimental study of 30 000 K_{e4} decays*

L. Rosselet, P. Extermann, J. Fischer, O. Guisan, R. Mermod, and R. Sachot†
University of Geneva, Geneva, Switzerland

A. M. Diamant-Berger, P. Bloch, G. Bunce,‡ B. Devaux, N. Do-Duc, G. Marel, and R. Turlay
Département de Physique des Particules Elémentaires, Centre d' Études Nucléaires, Saclay, France
(Received 26 August 1976)

An experiment on the decay $K^+ \to \pi^+\pi^-e^+\nu$ was performed at the CERN proton synchrotron with spark-chamber and counter techniques. The K_{e4} branching ratio has been measured relative to the τ decay. The $\pi\pi$ phase-shift difference $\delta_0^0 - \delta_1^1$ and the form factors of the hadronic current have been determined as functions of the $\pi\pi$ energy. The $\pi\pi$ scattering length a_0^0 has been evaluated from the phase shifts with a phenomenological model. The results are compared with the theoretical predictions of current algebra and other models.

I. INTRODUCTION

Among the various processes which have been proposed to study the $\pi\pi$ interaction at low energy, the K_{e4} decay ($K^+ \to \pi^+\pi^-e^+\nu$) has many interesting features. First of all the interaction occurs between two real pions which are the only hadrons in the final state and the only quantum states of the dipion which contribute to the decay are ($l=0$, $I=0$) and ($l=1$, $I=1$). Furthermore, the invariant-mass distribution of the dipion has a maximum relatively close to the $\pi\pi$ threshold. And, finally, the phenomenology of the weak interaction in terms of $V-A$ currents is sufficiently well understood to provide a reliable description of the decay. As a consequence, the phase-shift difference $\delta_0^0 - \delta_1^1$ can be extracted from the intensity distribution as a function of the dipion mass.

As was first demonstrated by Weinberg,[1] the form factors of the K-$\pi\pi$ axial-vector current can be related by current algebra to the K_{l3} form factors and to the pion decay amplitude. Weinberg gave also a prediction for the $\pi\pi$ scattering length a_0.[2] Therefore, the K_{e4} decay provides a good testing ground for current algebra and for the various techniques used in the extrapolation to the π mass shell.

Another point of interest, concerning the weak interaction, is the test of the $\Delta S = \Delta Q$ rule which forbids the decay $K^+ \to \pi^+\pi^+e^-\bar{\nu}$. This test gives the following result, as we reported in a previous paper[3]:

$$\Gamma(K_{e4}^+(e^-))/\Gamma(K_{e4}^+(e^+)) < 3.4\times 10^{-4} \quad (95\%\ \text{C.L.}) .$$

This supports the $\Delta S = \Delta Q$ rule very strongly.

The access to large K_{e4} samples, however, is difficult because of the very low branching ratio of this decay ($\sim 4\times 10^{-5}$). In the past, heavy-liquid bubble chambers produced a few hundred events.[4] More recently two counter experiments yielded larger statistics,[5,6] but the $\pi\pi$ scattering lengths obtained were barely compatible.

In this paper we present the results of a new experiment performed at CERN and subjected to two independent analyses.[7,8]

II. EXPERIMENT AND DATA REDUCTION

Apparatus

A top view of the experimental layout is shown in Fig. 1. The 2.8-GeV/c separated K^+ beam[9] was derived from an internal target of the CERN proton synchrotron. For a momentum bite of ±2%, intensities of 60 to 80×10^3 K^+'s over a 450-msec spill were obtained. The $K^+:\pi^+:p$ ratios were typically 1 : 2 : 0.4. Incident kaons (and protons) were tagged by the coincidence $S_1S_2\bar{C}_\pi\bar{A}$, where S_1 and S_2 refer to scintillation counters, C_π to a Cherenkov counter set to count pions, and A to a veto counter for the beam halo with a hole matching the beam profile. A high-pressure Cherenkov counter set to detect kaons was placed either in the decay zone for beam-tuning purposes or behind the apparatus as a relative monitor to check the stability of the separators.

The spectrometer[10,11] was designed to record kaons decaying into three charged particles (plus neutrals, if any) and to provide efficient electron identification. The 4-m-long decay zone was limited upstream by the proportional chamber PC_1, which measured the transverse coordinates of the incoming K^+, and downstream by the chamber PC_3, where a signal multiplicity corresponding to three particles was required by fast logics. An intermediate chamber PC_2 improved the measurement of the vertex. These three chambers had both horizontal and vertical sense wires with 2 mm spacing.

The momentum analysis of the decay particles

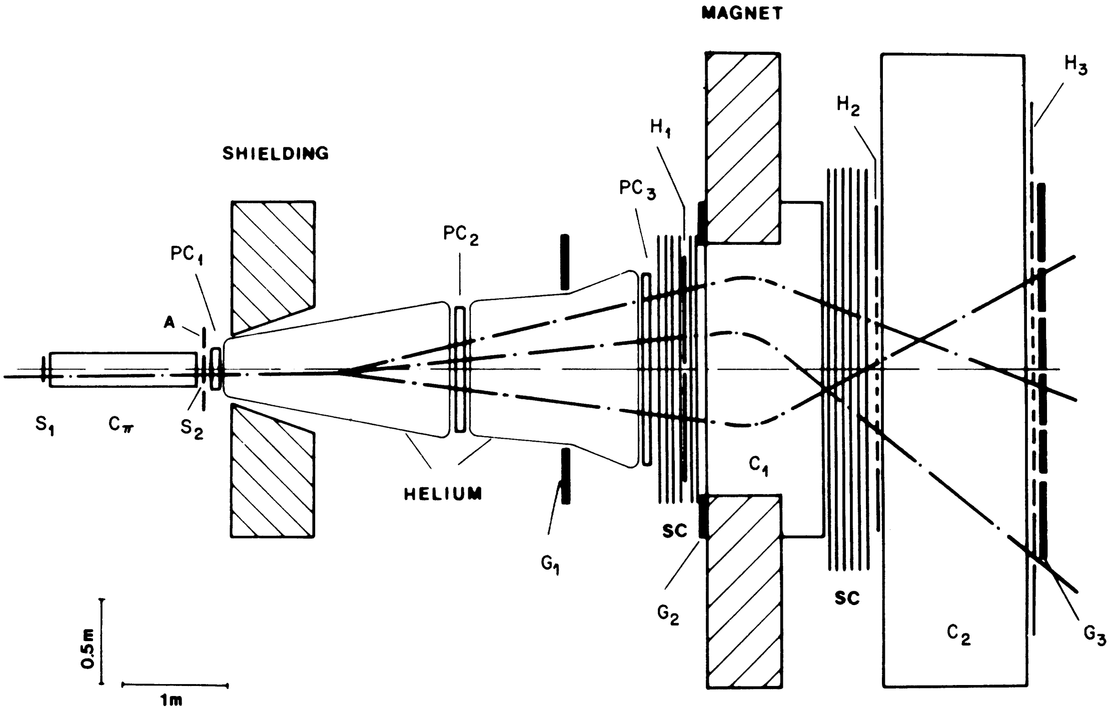

FIG. 1. A plan view of the experimental layout.

was made by a large-aperture-window-frame magnet (150×60 cm^2, 400 kG cm) and by two sets of six wire spark chambers with horizontal and vertical magnetostrictive readout.

The fast signal on the decay particles was given by three hodoscopes of scintillators, H_1, H_2, and H_3. The hodoscope H_1 was a wheel of 16 triangular elements with a 3-cm central hole on which the beam focused. H_2 and H_3 were symmetric arrays of 24 and 32 rectangular elements, respectively.

The electron identification was provided by two threshold Cherenkov counters, C_1 and C_2. The two counters were divided into 12 and 24 cells, respectively, and filled with isobutane at atmospheric pressure. The first counter was fitted into the magnet gap. The optical systems of the two counters were similar (see Fig. 2). The Cherenkov light was reflected by a cylindrical mirror on an array of semiparabolic light catchers with rectangular apertures. The relation between the trajectory of an incoming particle and the corresponding photomultipliers (PMs) was studied by Monte Carlo and checked experimentally. Since most of the time the particles were rather close together in C_1, the electron identification was mainly given by C_2.

Finally, the system included three γ-ray detectors G_1, G_2, and G_3, made of lead-scintillator sandwiches. The amount of material seen by the particles from the end of the decay zone to the entrance window of C_2 amounted to 0.04 radiation length.

The K_{e4} trigger was a coincidence between an incoming K^+, three charged particles in all three hodoscopes H_1, H_2, and H_3, and in the chamber PC_3, and at least one electron in each of the Cherenkov counters C_1 and C_2. These trigger conditions were met by the following main decay modes: $K^+\to\pi^+\pi^-e^+\nu$ (6% of the triggers), K^+ decays where a π^0 subsequently decayed into a Dalitz pair, i.e.,

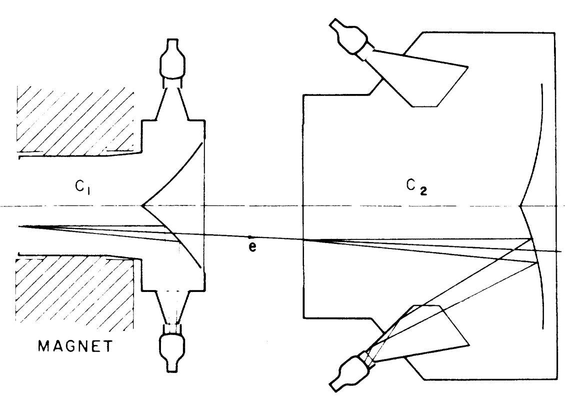

FIG. 2. A vertical section of the Cherenkov counters, parallel to the beam axis. The sides of the light catchers are parabolic cylinders.

$K^+ \to \pi^+\pi^0$ (32% of the triggers), $K^+ \to \pi^+\pi^0\pi^0$ (10%), $K^+ \to \pi^0\mu^+\nu$ (7%), $K^+ \to \pi^0 e^+\nu$ (4%). The contribution of τ decays with δ rays was strongly reduced by the coincidence between C_1 and C_2 and by the magnetic barrier. It amounted to 1%. The remaining triggers were due either to kaon decays with one of the secondaries interacting on the magnet pole pieces (13% of the triggers) or to kaon decays partially stopped by the magnetic barrier and combined with parasitic tracks (12%), or finally to interactions occuring before the decay zone or in the surrounding material (15%). It should be stressed that the decays with two or three electrons were not saturating the trigger and did not have to be rejected. This allowed the investigation of very rare K^+ decays, such as $K^+ \to \pi^+e^+e^-$,[12] $K^+ \to \pi^+\nu e^+e^-$, etc.,[13] with high sensitivity.

The data were transfered to a CII-9010 on-line computer by a CAMAC system and written on tape. Provision was made for a maximum rate of six events per burst. The computer stored the histograms needed for routine checks on the apparatus. It also provided a graphical display of the recorded events and an optical display of various scalers.

A total of 1.3×10^6 K_{e4} triggers were recorded in about 15 weeks of effective running time. The polarity of the analyzing magnet was reversed about every 10^5 triggers. For calibration, normalization, and alignment purposes different triggers were also recorded, mainly τ decays, with the magnet on (a few thousand every 10^4 K_{e4} triggers) and with the magnet off (every time the field was reversed).

Event reconstruction

The reconstruction program proceeded along the following steps. The signals of the spark chambers were associated with the signals of the proportional chamber PC_3 and of the hodoscopes H_2 and H_3. The horizontal and vertical projections were correlated by means of H_1, H_2, and H_3, and of two spark chambers with inclined wires. A consistent set of three trajectories was requested and a rough estimation of the momenta was made. The positions of the sparks were then corrected for the displacement due to the fringing field of the magnet (staggering). The signals of PC_1 and PC_2 were associated with the reconstructed event and the incident K^+ direction was determined. Then a constrained fit of the four trajectories to a single vertex was performed. Finally, the momenta of the secondary particles were determined from the field map and a code was assigned to each trajectory, depending on the signature of the Cherenkov counters. Kinematically constrained fits to various decay hypotheses could be requested: K_{e4}(1C), τ(4C), $K_{\pi 2}$-Dalitz(2C).

Reconstructed events were used for internal calibrations and for efficiency checks on the various detectors. Special attention was paid to the determination of the effective magnetic field by a fine adjustment of the effective K mass in τ decays.[11] The efficiency of the Cherenkov counter C_1 (which was in the magnet) was measured with K_{e3}-Dalitz decays identified by three electron signals in C_2. The e^+ of the weak decay was used as a probe. The mean efficiency of C_1 was found to be (93.8 ± 0.2)%. The efficiency of C_2 was determined with $K_{\pi 2}$-Dalitz decays identified by kinematics and was (99.7 ± 0.1)% on the average. The efficiency of C_1 and C_2 on pions was measured with τ decays. The probability for a pion to simulate an electron in both counters was $(2.0 \pm 0.2) \times 10^{-6}$.

Monte Carlo simulation

A detailed simulation of the apparatus provided Monte Carlo events in the same format as the true physical events. The various decays were generated in the c.m. system of the K^+, and transformed to the laboratory frame of reference. The incident trajectory and the vertex coordinates were chosen according to the beam profile. The decay products were traced through the magnet and affected by multiple Coulomb scattering, bremsstrahlung losses for the electrons, and decay in flight for the pions. Hits were generated in the chambers, the hodoscopes, and the Cherenkov counters, taking into account the resolution function of each detector as well as local inefficiencies, and then the trigger conditions were requested. Then the simulated events were processed through the same programs as the real events. Two independent Monte Carlo programs were written. Each one simulated about 3×10^5 K_{e4} decays.

Selection of the K_{e4} events and background

Before any kinematic requirement, the following sets of criteria and cuts were applied to the reconstructed K_{e4} triggers: (a) One and only one electron in the Cherenkov counters, and no hits in the γ counters G_1 and G_2. (G_3 was not used for the K_{e4} analysis.) (b) For each trajectory, a minimum number of sparks in each projection, good matching across the magnet and full agreement with the hodoscopes. (c) For the whole event, good χ^2 value of the vertex fit, no parasitic signal, neither in the hodoscopes nor in the Cherenkov counters, fiducial cuts on the decay volume, the magnet aperture, and the angles after the magnet.

From the 1.3×10^6 K_{e4} triggers, 540×10^3 could

TABLE I. Background computation. The asterisk (*) means that a factor of 2 is included for identical decay particles.

Decay mode	Branching ratio	Detection efficiency	Acceptance of cuts (a), (b), and (c)	Normalized product	Acceptance of kin. cuts	Final sample
K_{e4}	4.0×10^{-5}	0.104	0.75	32 869	0.914	30 036
τ(δ rays, PM noise)	5.6×10^{-2}	8.0×10^{-7}	0.80	758*	0.12	91
$\tau(\pi\to e\nu)$	6.9×10^{-6}	4.9×10^{-3}	0.17	116*	0.55	64
$\tau(\pi\to\mu\nu,\ \mu\to e\nu\nu)$	5.6×10^{-2}	1.1×10^{-6}	0.19	232*	0.33	76
$K_{\pi2}$-Dalitz	2.5×10^{-3}	4.7×10^{-5}	0.75	927	0.01	9
τ'-Dalitz	2.0×10^{-4}	4.5×10^{-5}	0.73	137*	0.13	18
$K_{\mu3}$-Dalitz	3.7×10^{-4}	6.0×10^{-5}	0.73	169	0.14	24
Total				35 208		30 318

be fully reconstructed (as expected from the trigger composition and the spectrometer efficiency), 86×10^3 met condition (a), and 32.5×10^3 met conditions (a), (b), and (c).

At this level, the contamination was evaluated from the Monte Carlo simulation and the experimental efficiencies. A K_{e4} event could be faked by the following decays: (i) τ with δ rays or accidentals in C_1 and C_2, and τ with subsequent $\pi\to e\nu$, or $\pi\to\mu\nu\to e\nu\bar{\nu}\nu$ decays. (ii) K^+ decays with a π^0 giving a Dalitz pair (mostly $K_{\pi2}$, $K_{\pi3}$, and τ'), where the e^- was not detected by C_2, and where the γ ray escaped G_1 and G_2.

In the sample of 35.2×10^3 events mentioned above, the total contribution of τ decays was 3.1%, and that of the Dalitz decays 3.5% (see Table I).

In order to reject the τ decays, we eliminated the events which satisfied the three following conditions: $p_{CT}<40$ MeV/c, $|\vec{p}_C-\vec{p}_K|<100$ MeV/c, and $|M_{\rm eff}(3\pi)-M_K|<20$ MeV, where $\vec{p}_C$ is the total momentum of the charged particles, $\vec{p}_K$ the incident momentum, and $p_{CT}=|\vec{p}_C\times\vec{p}_K|/|\vec{p}_K|$ the transverse-momentum balance. And in order to reject the Dalitz pairs, we requested $M_{\pi^+}>180$ MeV and $M_\nu^2>-10^4$ MeV, where M_{π^+} denotes the missing mass to the π^+ and M_ν^2 the effective neutrino mass squared in the K_{e4} hypothesis.

The remaining events were fitted to the K_{e4} kinematics and a cut was applied to the corresponding χ^2. The final K_{e4} sample contained 30 318 events. The contaminations by τ decays and Dalitz pairs were estimated to be 0.8% and 0.2%, respectively (see Table I). This background estimation was checked in different ways. First of all, the distribution of the transverse-momentum balance p_{CT} (Fig. 3) showed that the contamination due to the τ's was well below 2% and, in the same way, the effective mass distribution $M_{e^+e^-}$ (Fig. 3) gave

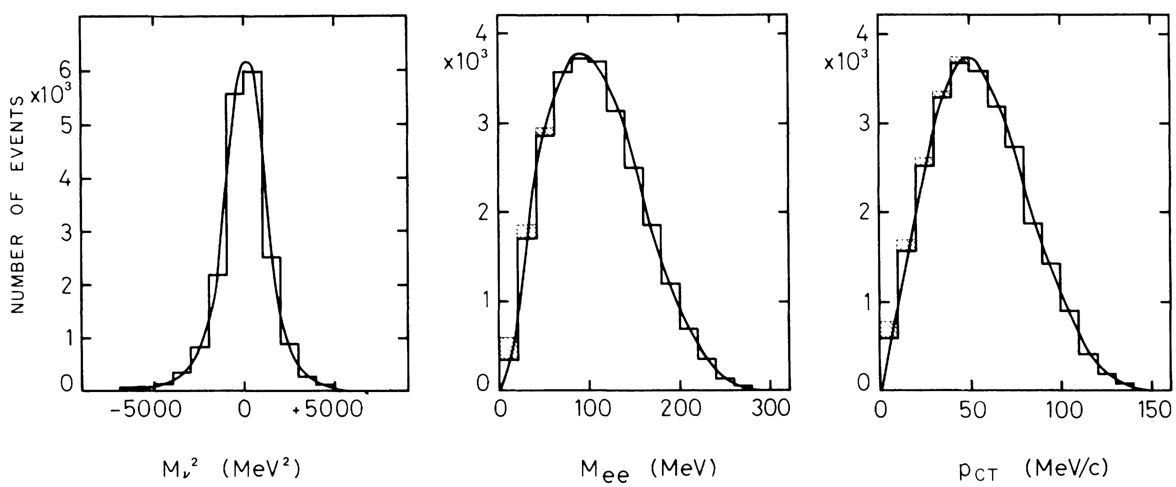

FIG. 3. Distribution of the effective mass squared of the neutrino in the K_{e4} hypothesis, of the e^+e^- effective mass in the Dalitz-pair hypothesis, and of the transverse-momentum balance of the charged particles. The histograms represent the K_{e4} events and the smooth curves the Monte Carlo simulation. The hatched areas on the M_{ee} and p_{CT} distributions correspond to an additional contamination of 2% by $K_{\pi2}$-Dalitz and τ decays, respectively.

an upper bound of 2% for the Dalitz pairs. A second check was made by Monte Carlo: a realistic mixture of K_{e4}, τ, and π^0-Dalitz events was processed through the kinematical cuts. The corresponding decrease of the Monte Carlo sample was exactly the same as for the experimental sample. A third check was provided by the number of $K_{e4}(e^-)$ candidates, 154, found with the same selection criteria, except for the sign of the electron. As was demonstrated in the study of the $\Delta S = \Delta Q$ rule (Ref. 3), those events were entirely due to background, mostly to τ decays where the π^- faked an e^-. Since the τ^+ decay gave $2\pi^+$ for $1\pi^-$, the background in the $K_{e4}(e^+)$ sample was expected to be of the order of 300 events, i.e. 1%, in close agreement with the calculation above.

For a part of the analysis, a special sample of 25 893 K_{e4} events was also used. It was obtained by more stringent requirements on the topology of the Cherenkov counters, on the χ^2 of the $K_{\pi 3}$ kinematic fit ($\chi^2 > 100$), and of the K_{e4} fit ($\chi^2 < 5$). The total contamination of this special sample was 0.3%.

Branching ratio

The K_{e4} branching ratio (R) was measured with respect to the branching ratio of the τ decay (R_τ). As it was explained before, τ decays were recorded at regular intervals between K_{e4} runs. The monitor was the number of coincidences $M = S_1 S_2 \bar{C}_\pi H_1 H_2 H_3$ (with three signals in each hodoscope), i.e., the number of K^+ decays into three charged particles. Let N be the number of reconstructed K_{e4} decays, selected by the above criteria and corrected for background, N_τ the number of τ selected by criteria (b) and (c), M and M_τ the corresponding monitor counts. Then the K_{e4} branching ratio is given by

$$R = R_\tau \frac{N}{M} \frac{M_\tau}{N_\tau} \frac{\epsilon_\tau}{\epsilon} ,$$

where ϵ_τ/ϵ is the ratio of the detection efficiencies of the two modes. The proportional chambers and the hodoscopes had the same efficiency for K_{e4} and τ decays. But it was found that the spark chambers were about 3% less efficient for τ decays (6 triggers/burst) than for K_{e4} decays (~0.5 trigger/burst) and this effect was taken into account.

For the study of the branching ratio, relatively short periods were selected, where the beam separators as well as the overall detection efficiency of the apparatus had optimum stability. This corresponds to about 10% of the data.

With $R_\tau = (5.59 \pm 0.03) \times 10^{-2}$,[14] the K_{e4} branching ratio was found to be

$$R = (4.03 \pm 0.18) \times 10^{-5} .$$

A systematic error of 3% was included in the error. This result is in good agreement with Refs. 5 and 14.

The $K_{e4}/K_{\pi 2}$-Dalitz ratio was also studied. This method should have some advantages over the previous one because the $K_{\pi 2}$ and the K_{e4} were recorded at the same time with the same trigger. But, due to the fact that the two electrons of the Dalitz pair were emitted with a very small opening angle, the detection efficiency was very sensitive to slight fluctuations in the resolution of the spark chambers. As a consequence this method turned out to be less reliable than the normalization to τ decays but, nevertheless, it gave compatible results.

III. METHODS OF ANALYSIS

Configuration variables and transition probability

The K_{e4} decay is usually described by a set of five configuration variables introduced by Cabibbo and Maksymowicz[15]: $s_\pi = M_{\pi\pi}{}^2$ and $s_l = M_{e\nu}{}^2$ the invariant squared masses, and the three angles θ_π, θ_l, and ϕ as defined in Fig. 4.

The transition amplitude given by the $V-A$ theory can be written as[16]:

$$(G_w/\sqrt{2}) \sin\theta_C \langle \pi^+\pi^- | A^\lambda + V^\lambda | K^+ \rangle \bar{u}_\nu \gamma_\lambda (1-\gamma_5) v_e ,$$

where

$$\langle \pi^+\pi^- | A^\lambda | K^+ \rangle = \frac{1}{m_K} [F(p_{\pi^+} + p_{\pi^-}) + G(p_{\pi^+} - p_{\pi^-}) + R(p_K - p_{\pi^+} - p_{\pi^-})]^\lambda \qquad (1)$$

and

$$\langle \pi^+\pi^- | V^\lambda | K^+ \rangle = \frac{1}{m_K{}^3} H \epsilon^{\lambda\mu\nu\rho} (p_K)_\mu (p_{\pi^+} + p_{\pi^-})_\nu \times (p_{\pi^+} - p_{\pi^-})_\rho$$

are the matrix elements for the axial-vector and vector hadronic currents, respectively. In these expressions p denotes the momentum four-vector of each particle.

The form factors F, G, H, and R are dimensionless complex functions of s_π, s_l, and $\cos\theta_\pi$.

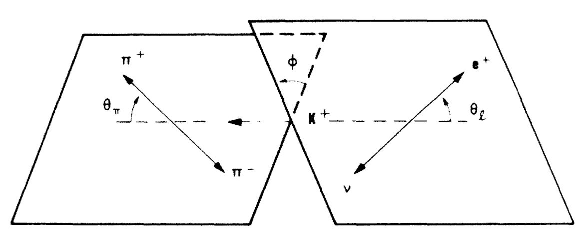

FIG. 4. Configuration variables of the K_{e4} decay. The angle θ_π is defined in the c.m. of the dipion, θ_l in the c.m. of the dilepton, and ϕ in the c.m. of the K^+.

The form factor R cannot be determined from the K_{e4} decay because its contribution to the decay probability is multiplied by m_e^2/s_l and therefore is negligible.

Pais and Treiman have shown[16] that the form factors enter into the decay probability through the following combinations:

$$F_1=\gamma F+\alpha G\cos\theta_\pi ,$$
$$F_2=\beta G , \qquad (2)$$
$$F_3=\beta\gamma H/m_K^2 ,$$

with[17]

$$\alpha=\tfrac{1}{2}(m_K-s_\pi-s_l)\left(\frac{s_\pi-4m_\pi^2}{s_\pi}\right)^{1/2} ,$$
$$\beta=[(s_\pi-4m_\pi^2)s_l]^{1/2} ,$$
$$\gamma=[\tfrac{1}{4}(m_K^2-s_\pi-s_l)^2-s_\pi s_l]^{1/2} ,$$

and that the probability distribution has a simple expansion in the $\cos\theta_l\times\phi$ plane:

$$d^5\Gamma=\frac{\pi^2}{(2\pi)^8}\frac{G_w^2\sin^2\theta_C}{16m_K^5}\left(\frac{s_\pi-4m_\pi^2}{s_\pi}\right)^{1/2}I(s_\pi,s_l,\cos\theta_\pi,\cos\theta_l,\phi)ds_\pi ds_l d\cos\theta_\pi d\cos\theta_l d\phi , \qquad (3)$$

where

$$I=I_1+I_2\cos2\theta_l+I_3\sin^2\theta_l\cos2\phi+I_4\sin2\theta_l\cos\phi+I_5\sin\theta_l\cos\phi$$
$$+I_6\cos\theta_l+I_7\sin\theta_l\sin\phi+I_8\sin2\theta_l\sin\phi+I_9\sin^2\theta_l\sin2\phi . \qquad (4)$$

The complete expressions for the coefficients I_i as functions of F_1, F_2, F_3, and θ_π are given in Ref. 16.

We can write the θ_π dependence of the form factors explicitly by making a partial-wave expansion of the hadronic current with respect to the angular momentum of the dipion system:

$$F=f_s\exp(i\delta_s)+f_p\exp(i\delta_p)\cos\theta_\pi$$
$$+d\text{-wave term}+\cdots ,$$
$$G=g\exp(i\delta_g)+d\text{-wave term}+\cdots , \qquad (5)$$
$$H=h\exp(i\delta_h)+d\text{-wave term}+\cdots .$$

Because of the small values of s_π in the K_{e4} decay, these expansions may be restricted to s and p waves. Note that the first term in the expansion of G and H corresponds to a p wave. After a rotation by the phase angle δ_g and with the notation $\delta=\delta_s-\delta_g$, $\omega=\delta_p-\delta_g$, $\omega_2=\delta_h-\delta_g$, the functions F_1, F_2, and F_3 become

$$F_1=\gamma f_s\exp(i\delta)+\cos\theta_\pi[\alpha g+\gamma f_p\exp(i\omega)],$$
$$F_2=\beta g , \qquad (6)$$
$$F_3=\beta\gamma h/m_K^2\exp(i\omega_2) .$$

As pointed out in previous measurements,[4,5] the experimental determinations of f_p and g are strongly correlated. This is due to the fact that f_p contributes to the decay probability through F_1 only, in combination with g. In order to avoid this problem, we introduce a new form factor

$$g'\exp(i\omega_1)=g+(\gamma/\alpha)f_p\exp(i\omega) , \qquad (7)$$

which is not correlated to g. The magnitude of f_p is then proportional to the difference between g and g'.

With the expressions (6) and (7), we obtain for the function I the following expansion:

$$2I=\sum_{k=1}^{15}A_k(f_s,g,g',h,\delta,\omega_1,\omega_2)$$
$$\times B_k(s_\pi,s_l,\cos\theta_\pi,\cos\theta_l,\phi) . \qquad (8)$$

The functions A_k and B_k are given in Table II.

If T invariance holds, the Fermi-Watson theorem implies that the phases in the partial wave expansion (5) are the phase shifts of the elastic $\pi\pi$ scattering. Furthermore, we shall assume that the $\Delta I=\frac{1}{2}$ rule suppresses the $(l=0,I=2)$ partial wave. As a consequence, we obtain

$$\delta_s=\delta_0^0,$$
$$\delta_p=\delta_g=\delta_h=\delta_1^1,$$
$$\delta=\delta_0^0-\delta_1^1,$$

and

$$\omega_1=\omega_2=0.$$

Acceptance, resolution, and binning

In order to compare the experimental and theoretical distributions in the configuration space, we have to take into account the acceptance and resolution functions of the apparatus. These functions are evaluated by Monte Carlo techniques. The integrated distributions of the acceptance $\epsilon(s_\pi, s_l, \cos\theta_\pi, \cos\theta_l, \phi)$, shown in Fig. 5, demonstrate that the whole phase space is accessible with good efficiency, except for $\cos\theta_l$ close to -1 or for $M_{\pi\pi}$ above 430 MeV. The errors of reconstruction on the configuration variables are as follows: $\sigma(M_{\pi\pi})=2.2$ MeV, $\sigma(M_{e\nu})=5.5$ MeV, $\sigma(\cos\theta_\pi)=0.05$, $\sigma(\cos\theta_l)=0.05$, and $\sigma(\phi)=0.14$ rad.

TABLE II. Functions entering the expansion of the probability distribution [see Eq. (8)].

k	A_k	B_k	A'_k
1	f_s^2	$\gamma^2\sin^2\theta_l$	N
2	g'^2	$\alpha^2\cos^2\theta_\pi\sin^2\theta_l$	$N\bar{g}'^2R_1$
3	g^2	$\beta^2\sin^2\theta_\pi(1-\sin^2\theta_l\cos^2\phi)$	$N\bar{g}^2R_2$
4	h^2	$(\beta^2\gamma^2/M_K^4)\sin^2\theta_\pi(1-\sin^2\theta_l\sin^2\phi)$	$N\bar{h}^2R_3$
5	$f_sg'\cos(\delta-\omega_1)$	$2\alpha\gamma\cos\theta_\pi\sin^2\theta_l$	$N\bar{g}'\cos(\delta-\omega_1)$
6	$f_sg\cos\delta$	$\beta\gamma\sin\theta_\pi\sin2\theta_l\cos\phi$	$N\bar{g}\cos\delta$
7	$f_sh\cos(\delta-\omega_2)$	$-(2/M_K^2)\beta\gamma^2\sin\theta_\pi\sin\theta_l\cos\phi$	$N\bar{h}\cos(\delta-\omega_2)$
8	$g'g\cos\omega_1$	$\frac{1}{2}\alpha\beta\sin2\theta_\pi\sin2\theta_l\cos\phi$	$N\bar{g}'\bar{g}R_4\cos\omega_1$
9	$g'h\cos(\omega_2-\omega_1)$	$-(1/M_K^2)\alpha\beta\gamma\sin2\theta_\pi\sin\theta_l\cos\phi$	$N\bar{g}'\bar{h}R_5\cos\omega_3$
10	$gh\cos\omega_2$	$-(2/M_K^2)\beta^2\gamma\sin^2\theta_\pi\cos\theta_l$	$N\bar{g}\bar{h}R_6\cos\omega_4$
11	$f_sg\sin\delta$	$2\beta\gamma\sin\theta_\pi\sin\theta_l\sin\phi$	$N\bar{g}\sin\delta$
12	$f_sh\sin(\delta-\omega_2)$	$-(1/M_K^2)\beta\gamma^2\sin\theta_\pi\sin2\theta_l\sin\phi$	$N\bar{h}\sin(\delta-\omega_2)$
13	$g'g\sin\omega_1$	$\alpha\beta\sin2\theta_\pi\sin\theta_l\sin\phi$	$N\bar{g}'\bar{g}R_4\sin\omega_1$
14	$g'h\sin(\omega_2-\omega_1)$	$(1/2M_K^2)\alpha\beta\gamma\sin2\theta_\pi\sin2\theta_l\sin\phi$	$N\bar{g}'\bar{h}R_5\sin\omega_3$
15	$gh\sin\omega_2$	$-(1/M_K^2)\beta^2\gamma\sin^2\theta_\pi\sin^2\theta_l\sin2\phi$	$N\bar{g}\bar{h}R_6\sin\omega_4$

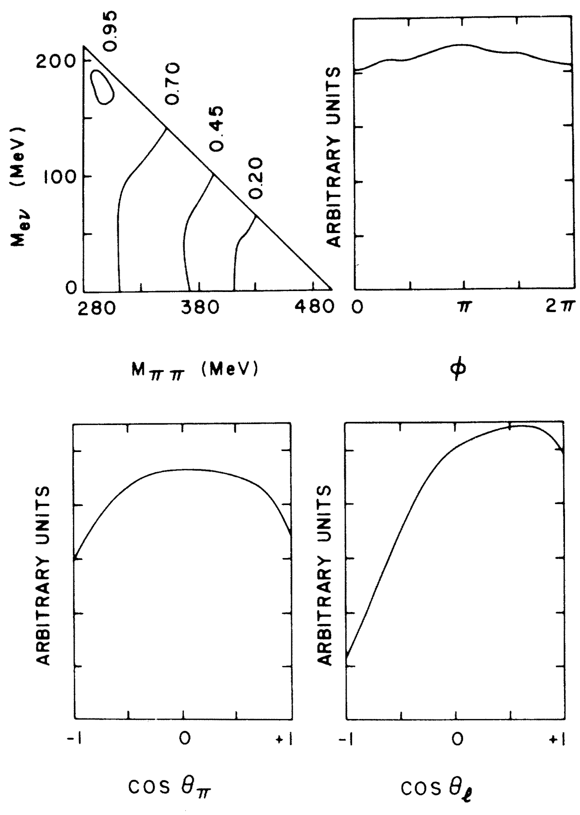

FIG. 5. One- and two-dimensional plots of the acceptance function $\epsilon(s_\pi, s_l, \cos\theta_l, \phi)$ integrated over the other variables.

When the physical parameters and the kinematic variables can be separated as in Eq. (8), the most economical way to evaluate the probability of finding an event in a given region of phase space is to use weights computed by Monte Carlo techniques.[18] One defines a certain number of bins and for each bin one computes the average values $\langle \epsilon B_k \rangle$. This method allows one to take into account the resolution function, but it requires a binning of the data which could reduce the amount of physical information. The number and the size of the five-dimensional bins are optimized according to the dependence of $d^5\Gamma$ on each variable. We define eight bins in ϕ (the highest term is $\sin 2\phi$), five bins in $\cos\theta_\pi$ (highest term $\sin^2\theta_\pi$), five bins in $\cos\theta_l$ (highest term $\sin 2\theta_l$), five bins in $M_{\pi\pi}$, and three in $M_{e\nu}$, i.e., a total of 3000 bins. The populations of the 15 bins in the $M_{\pi\pi} \times M_{e\nu}$ plane are about equal.

For a given set of parameters, the comparison is usually made with a χ^2 estimator. In our case however, this estimator cannot be used because the mean number of events per bin is only 10. Therefore, we replace it by other estimators which take into account the Poisson fluctuations of both experimental and Monte Carlo events.[7,8]

Extraction of form factors and phase shifts

At a time when only small samples of K_{e4} decays were available, Pais and Treiman[16] proposed an elegant method to extract the phase shift

δ with minimal *a priori* assumptions about the form factors. The idea was to integrate the probability distribution $d^5\Gamma$ over the variables s_π, s_l, and $\cos\theta_\pi$ and to fit it to the event distribution in the $\cos\theta_l \times \phi$ plane, using the coefficients

$$\langle I_i \rangle = \int\int\int I_i \, ds_\pi \, ds_l \, d\cos l_\pi$$

as free parameters. The phase shift δ was given by

$$\tan\delta = \frac{1}{2}\frac{\langle I_7 \rangle}{\langle I_4 \rangle} \quad \text{or} \quad \tan\delta = 2\frac{\langle I_8 \rangle}{\langle I_5 \rangle}.$$

This method, however, was devised for an ideal detector with a uniform efficiency over the whole phase space. In order to use it with a realistic apparatus, one has to introduce the acceptance function ϵ and, furthermore, to factorize it in the following way[19]:

$$\epsilon(s_\pi, s_l, \cos\theta_\pi, \cos\theta_l, \phi) = \epsilon_1(s_\pi, s_l, \cos\theta_\pi) \times \epsilon_2(\cos\theta_l, \phi).$$

But at the present level of statistical accuracy, the acceptance of our apparatus cannot be factorized without introducing a significant bias. Indeed, it can be seen from Fig. 6 that the acceptance produces a correlation between ϕ and $\cos\theta_\pi$.

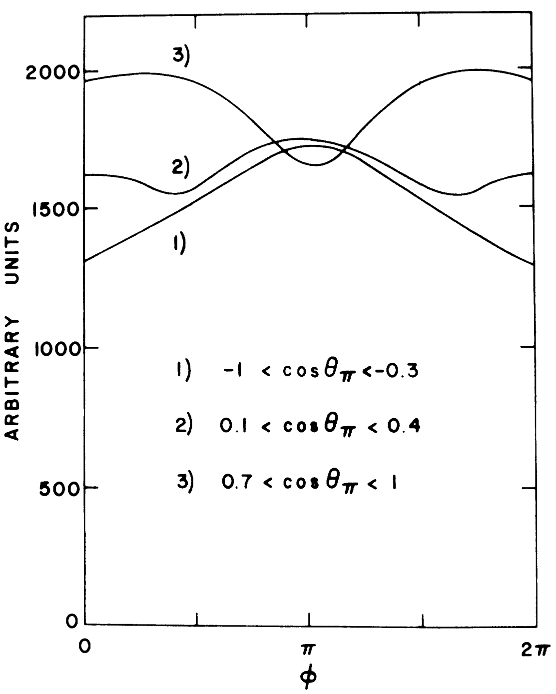

FIG. 6. One-dimensional plots of the acceptance function ϵ integrated over s_π, s_l, $\cos\theta_l$, and different intervals in $\cos\theta_\pi$. This demonstrates that ϵ cannot be factorized as $\epsilon_1(s_\pi, s_l, \cos\theta_\pi) \times \epsilon_2(\cos\theta_l, \phi)$.

As a consequence, we shall use an extension of the original Pais-Treiman method to the whole configuration space, without projection on any subspace. In this way, we take full advantage of the large statistics available. We take the probability distribution given by Eqs. (3) and (8) and multiplied by the acceptance function $\epsilon(s_\pi, s_l, \cos\theta_\pi, \cos\theta_l, \phi)$, and we fit it to the data with the 15 coefficients A_k as independent parameters. The phases δ, ω_1, and ω_2 are given by the relations

$$\begin{aligned} &\tan\delta = A_{11}/A_6, \\ &\tan(\delta - \omega_2) = A_{12}/A_7, \\ &\tan\omega_1 = A_{13}/A_8, \\ &\tan(\omega_2 - \omega_1) = A_{14}/A_9, \\ &\tan\omega_2 = A_{15}/A_{10}. \end{aligned} \tag{9}$$

As mentioned before, T invariance implies $\omega_1 = \omega_2 = 0$ and can be checked from the relations

$$A_{11}/A_6 = A_{12}/A_7 \quad \text{and} \quad A_{13} = A_{14} = A_{15} = 0.$$

The coefficients A_k carry also the information on the form factors. This information, however, is quite redundant, since the same form factor can be obtained from different combinations of A_k (see Table II). For technical reasons we define a new set of 15 parameters A_k', given in the last column of Table II: four physical parameters ($\bar{g} = \bar{g}/f_s$, $\bar{g}' = g'/f_s$, $\bar{h} = h/f_s$, and δ), one normalization factor N proportional to f_s^2, four phases ω_i which should be equal to zero by T invariance, and six quantities R_j which must be equal to 1 for internal consistency. By fixing all the ω_i and R_j to their expected values, we can perform a fit with the usual four parameters of the K_{e4} decay. By releasing some of the ω_i and R_j, we obtain a fit with any number of free parameters between 4 and 14. This provides us with an efficient tool for detecting discrepancies between the experimental and theoretical distributions.

Search for systematic errors

Since the Monte Carlo simulation is a crucial part of our analysis, it is of prime importance to check it in many different ways. We compare the lab distributions of the particle momenta and angles, the distributions of impact points on various planes, etc. The vertex position along the beam axis and the momenta of the charged decay products are presented on Fig. 7. Note that realistic values of the form factors and phase shifts are included in the Monte Carlo. But the lab distributions are not very sensitive to the actual value of the parameters. Furthermore, we make the same comparison with τ decays and the agreement is also quite good. For K_{e4} decays, the effective mass squared of the neutrino (see Fig. 3) provides a sensitive check of the resolution.

The internal consistency of the data is verified by comparing different subsamples: one magnet polarity against the other, different production periods, decays occurring upstream and downstream of PC_2, etc. In every case, the differences never exceed one statistical standard deviation for $\bar{g}$, $\bar{g}'$ and δ and two deviations for $\bar{h}$.

The effect of the contamination by τ decays deserves special attention. As explained before, this contamination amounts to 0.8%. If we take a sample of simulated K_{e4} events with this admixture of τ decays, we observe the following effects. In a search with 14 parameters, R_2 and R_3 increase by about 2 standard deviations above their expected values, but $\bar{g}$, $\bar{g}'$, $\bar{h}$, δ, and N remain practically unchanged. In a four parameter search, however, g increases and δ decreases about 1 standard deviation each. The stability of the physical parameters can be recovered by releasing R_2 and R_3, i.e., by performing a six-parameter search. This behavior can be understood from the fact that the τ's have a tendency to cluster in a certain band of the $M_{\pi\pi}\times M_{e\nu}$ plane at $M_{e\nu}\simeq m_\pi$. In order to avoid this bias, we use two different procedures. In the first one, we subtract the background by adding an appropriate percentage of τ's to the theoretical K_{e4} sample, and we perform a six-parameter search. In the second one, we apply more restrictive cuts which reduce the background to 0.3% (see above) and we perform a four-parameter search with 25 893 events. The two procedures give compatible results.

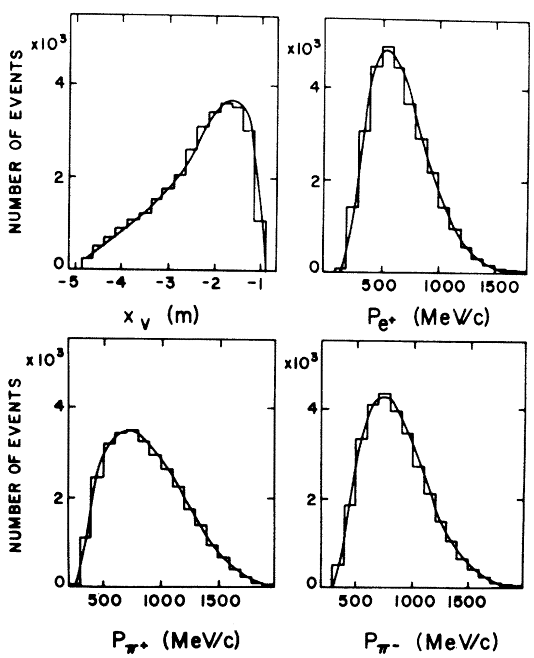

FIG. 7. Distribution of the vertex along the beam, and of the π^+, π^-, and e^+ momenta. (Histogram: K_{e4} events; smooth curve: Monte Carlo simulation.)

Systematic errors could also originate from certain processes which are not included in the decay probability (3).

For the evaluation of the radiative corrections, we use calculations similar to those performed by E. Ginsberg[20] for the K_{l3} decay modes. We introduce those corrections in the probability distribution (3), we generate Monte Carlo events according to this new distribution and to the acceptance function, and we process them as normal events. We observe an effect mainly on the $M_{\pi\pi}$ distribution (classical Coulomb interaction between the two pions) and on the $\cos\theta_\pi$ distribution [as pointed out in Ref. 6]. These corrections are included in the final results, but their effect is quite small: the form factor $\bar{h}$ is decreased by 0.10 and the factor N slightly increased at low values of $M_{\pi\pi}$.

We have no means of checking the $\Delta I=\frac{1}{2}$ rule. Transitions with $\Delta I=\frac{3}{2}$ introduce $I=2$ terms in f_s which have the same dependence on the kinematical variables as the $I=0$ terms and therefore cannot be disentangled. The only possibility would be to compare $K^+\to\pi^+\pi^-e^+\nu$ and $K^+\to\pi^0\pi^0e^+\nu$ decays.[16] According to what is known from other semileptonic decays, the $\Delta I=\frac{1}{2}$ rule should be valid at least to the 90% level. The effect of a 10% violation on the phase shift δ is smaller than one statistical standard deviation.

Pais and Treiman also proposed to test the locality of the coupling between the lepton pair and the hadronic current. We find that the theoretical distribution [Eq. (3) and (8)], where locality is assumed, fitted the data very well and we conclude therefore that this hypothesis is valid, at least up to the level of the radiative corrections.

IV. RESULTS

The results of the two independent analyses are perfectly compatible. Therefore we are presenting here for each point the average of the two values obtained, with the larger of the two error bars.

Relative form factors

The values of $\bar{g}$, $\bar{g}'$, and $\bar{h}$ are given in Table III for the five bins in $M_{\pi\pi}$. We do not observe any energy dependence. The mean values over the five bins are

$$\langle\bar{g}\rangle=0.855\pm0.041,$$

TABLE III. Relative form factors and phase shifts for the five bins in $M_{\pi\pi}$.

$M_{\pi\pi}$ (MeV)	280–296	296–310	310–325	325–347	>347
Number of events	5673	6128	5941	6472	6108
$\langle M_{\pi\pi}\rangle$ (MeV)	289	303	317	335	367
N	0.967 ± 0.03	0.955 ± 0.014	0.981 ± 0.015	1.004 ± 0.015	1.047 ± 0.016
$\bar{g}$	0.83 ± 0.18	0.81 ± 0.11	0.93 ± 0.09	0.78 ± 0.08	0.89 ± 0.07
$\bar{g}'$	0.90 ± 0.07	0.89 ± 0.05	0.89 ± 0.04	0.81 ± 0.04	0.88 ± 0.04
$\bar{h}$	−0.77 ± 0.40	−0.59 ± 0.26	−0.37 ± 0.21	−0.40 ± 0.24	−0.54 ± 0.32
δ(rad)	0.07 ± 0.13	0.21 ± 0.07	0.13 ± 0.05	0.20 ± 0.04	0.27 ± 0.04

$$\langle \bar{g}'\rangle = 0.868 \pm 0.020,$$

$$\langle \bar{h}\rangle = -0.48 \pm 0.12.$$

The difference between $\langle \bar{g}\rangle$ and $\langle \bar{g}'\rangle$, which is proportional to f_p, is compatible with zero. This means that the form factor F is contributing to the s wave only. In Table IV, these results are compared with the two previous experiments. The agreement is quite good except perhaps for f_p, which according to Beier *et al.* was 2 standard deviations away from zero.

The normalization factor N, also given in Table III, exhibits a slight increase with $M_{\pi\pi}$. Since N is proportional to $f_s^2/\langle f_s^2\rangle$, we can refer this variation to an energy dependence of f_s, which we write in the following way:

$$f_s(q^2) = f_s(0)(1+\lambda q^2), \tag{10}$$

where $q = [(s_\pi - 4m_\pi^2)/4m_\pi^2]^{1/2}$ is the pion momentum in the dipon c.m. system. We find

$$\lambda = 0.08 \pm 0.02.$$

This is the first evidence for a variation of a form factor in the energy range of the K_{e4} decay. According to Morgan and Pennington,[21] it is not possible to relate this slope λ to the s-wave $\pi\pi$ scattering length a_0 by means of the Watson enhancement factor.[4]

Considering now the other energy variable $M_{e\nu}$, we do not observe any significant dependence of the form factors.

Decay rate and absolute form factors

From the branching ratio measured in this experiment and the tabulated K^+ lifetime[14] we obtain the following K_{e4} decay rate:

$$\Gamma = (3.26 \pm 0.15)\times 10^3 \text{ sec}^{-1}.$$

Normalizing the form factors to this rate, we find

$$f_s(0)\sin\theta_C = 1.23 \pm 0.03,$$

$$g(0)\sin\theta_C = 1.05 \pm 0.06,$$

$$h(0)\sin\theta_C = -0.59 \pm 0.15,$$

where θ_C is the Cabibbo angle.

The theoretical situation was reviewed by Chounet, *et al.*[22] The predictions of current algebra, assuming constant form factors, are

$$|f_s \sin\theta_C| = |g \sin\theta_C| = 0.80 \pm 0.02.$$

Different models[23] have been used to take into account an energy dependence of the form factors. They yield

$$0.55 \lesssim g/f_s \lesssim 1.22.$$

Our results are in reasonable agreement with those predictions and it might be worthwhile now to include the observed energy dependence of f_s in the calculations.

Various estimations obtained from strong-interaction diagrams with SU(3) coupling constants give rather loose predictions for h (see Ref. 22):

$$0.3 \lesssim |h \sin\theta_C| \lesssim 1,$$

in agreement with the experiment.

Time-reversal invariance

As we have seen before, T invariance implies that the p-wave form factors g, g', and h should

TABLE IV. Average values of the relative form factors and phase shifts found by Basile *et al.* (Ref. 5), Beier *et al.* (Ref. 6), and in this experiment. The χ^2 refer to overall fits.

Experiment	Basile *et al.*	Beier *et al.*	This experiment
Number of events	1609	8141	30318
$\langle \bar{f}_p\rangle$	−0.049 ± 0.072	0.077 ± 0.037	0.009 ± 0.032
$\langle \bar{g}\rangle$	0.86 ± 0.14	0.86 ± 0.05	0.855 ± 0.041
$\langle \bar{h}\rangle$	−0.97 ± 0.46	−0.71 ± 0.23	−0.48 ± 0.12
$\langle\delta\rangle$ (rad)	0.34 ± 0.13	0.19 ± 0.05	0.205 ± 0.022
χ^2/DF	47/35	67/54	2957/2982

have the same phase, i.e., $\omega_1 = \omega_2 = 0$. A search with ω_1 and ω_2 free gives the following result, averaged over the 5 bins in $M_{\pi\pi}$:

$$\langle \omega_1 \rangle = 0.05 \pm 0.07,$$

$$\langle \omega_2 \rangle = 0.14 \pm 0.22,$$

in good agreement with time-reversal invariance.

d-wave contribution

The expansion of the form factors (5) has been limited to *s* and *p* waves. In order to check this approximation we add a *d*-wave term to G:

$$G = g_p \exp(i\delta_1^1) + g_d \exp(i\delta_2^0)\cos\theta_\pi .$$

We find $\bar{g}_d$ $(=g_d/f_s)$ compatible with zero, even in the highest bin in $M_{\pi\pi}$, and we obtain the average value

$$\langle \bar{g}_d \rangle = 0.04 \pm 0.04.$$

$\pi\pi$ phase shifts

The phase-shift difference $\delta = \delta_0^0 - \delta_1^1$ for the five bins in $M_{\pi\pi}$ is given in the last row of Table III. It is also plotted in Fig. 8, along with the points of the two previous K_{e4} experiments. Concerning the discrepancy between Zylbersztejn *et al.* and Beier *et al.* at 320 MeV, one can see that our new points give an intermediate value which is compatible with either experiment.

Correcting δ for the small contribution of δ_1^1 ($<1°$, Ref. 24), we obtain the phase shift δ_0^0 and we compare it in Fig. 9 to the data of the pion-production experiments. There is good agreement with the two $\pi^+\pi^-$ experiments[25,26] which have points below 500 MeV. However, most of the data from $\pi^0\pi^0$ production[28] are significantly higher.

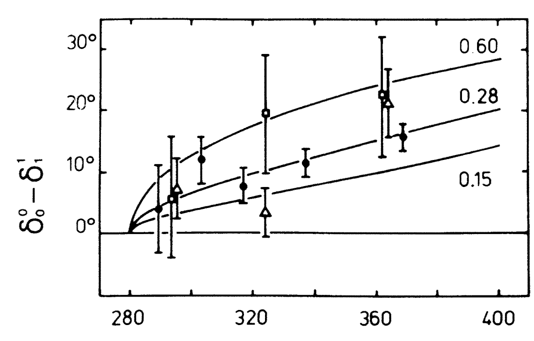

FIG. 8. Phase-shift difference $\delta_0^0 - \delta_1^1$ from K_{e4} experiments: Zylbersztejn *et al.* (Ref. 5) (squares), Beier *et al.* (Ref. 6) (triangles) and this experiment (circles). The curves are given by Eq. (11) for different values of the scattering length a_0^0.

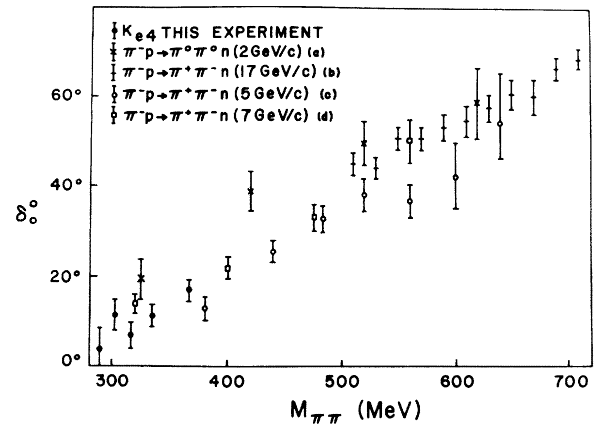

FIG. 9. Phase shift δ_0^0 from K_{e4} decay and from π production: (a) Ref. 28, (b) Ref. 27, (c) Ref. 26, (d) Ref. 25.

Scattering length

In order to compute the *s*-wave scattering length a_0^0, we use the model of Basdevant, Froggatt, and Petersen.[24] This model provides solutions to Roy's equations which fit the $\pi\pi$ phase shifts between 500 and 900 MeV. In the energy range of the K_{e4} decay these solutions can be approximated by the following expansion:

$$\sin 2\delta = 2\left(\frac{s_\pi - 4m_\pi{}^2}{s_\pi}\right)^{1/2}(a_0^0 + bq^2/m_\pi{}^2), \qquad (11)$$

where $b = b_0^0 - a_1^1$, i.e., the difference between the *s*-wave slope and the *p*-wave scattering length. According to the model of Basdevant *et al.*, b and a_0^0 are related by the expression

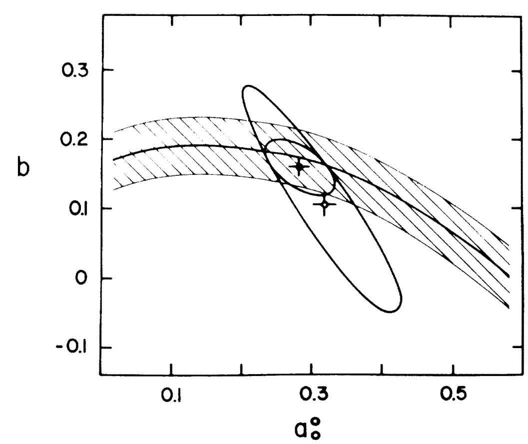

FIG. 10. Results of the fit of formula (11) to the five points of δ. The open circular point and the large error ellipse correspond to the two-parameter fit, whereas the black dot and the small ellipse correspond to the one-parameter fit with b constrained by Eq. (12). Thi constraint is represented by the hatched band.

$$b = 0.19 - (a_0^0 - 0.15)^2, \tag{12}$$

with a theoretical uncertainty of ±0.04 on b. The expected behavior of δ for different values of a_0^0 is shown by the curves in Fig. 8.

One way to determine a_0^0 is to fit Eq. (11) to the five values of δ. With a_0^0 and b as free parameters, we obtain $a_0^0 = 0.31 \pm 0.11$ and $b = 0.11 \pm 0.16$, as shown by the large ellipse in Fig. 10. With b constrained by Eq. (12) (shaded band on that figure), we find

$$a_0^0 = 0.28 \pm 0.05,$$

as shown by the small ellipse on Fig. 10.

An alternative way is to introduce the expansions (10) and (11) in the probability density (3) and to make an overall fit to the data with λ, $\bar{g}$, $\bar{g}'$, h, and a_0^0 as free parameters. This gives exactly the same results and the agreement between the fit and the observed distributions is excellent (see Fig. 11).

The final value of the scattering length a_0^0 sits well within the bounds given by the conditions of analyticity, unitarity, and crossing symmetry.[24] It is somewhat above the original Weinberg prediction, but it appears that this prediction can be revised without any fundamental change in current algebra or in the partial conservation of axial-vector current.[29,30]

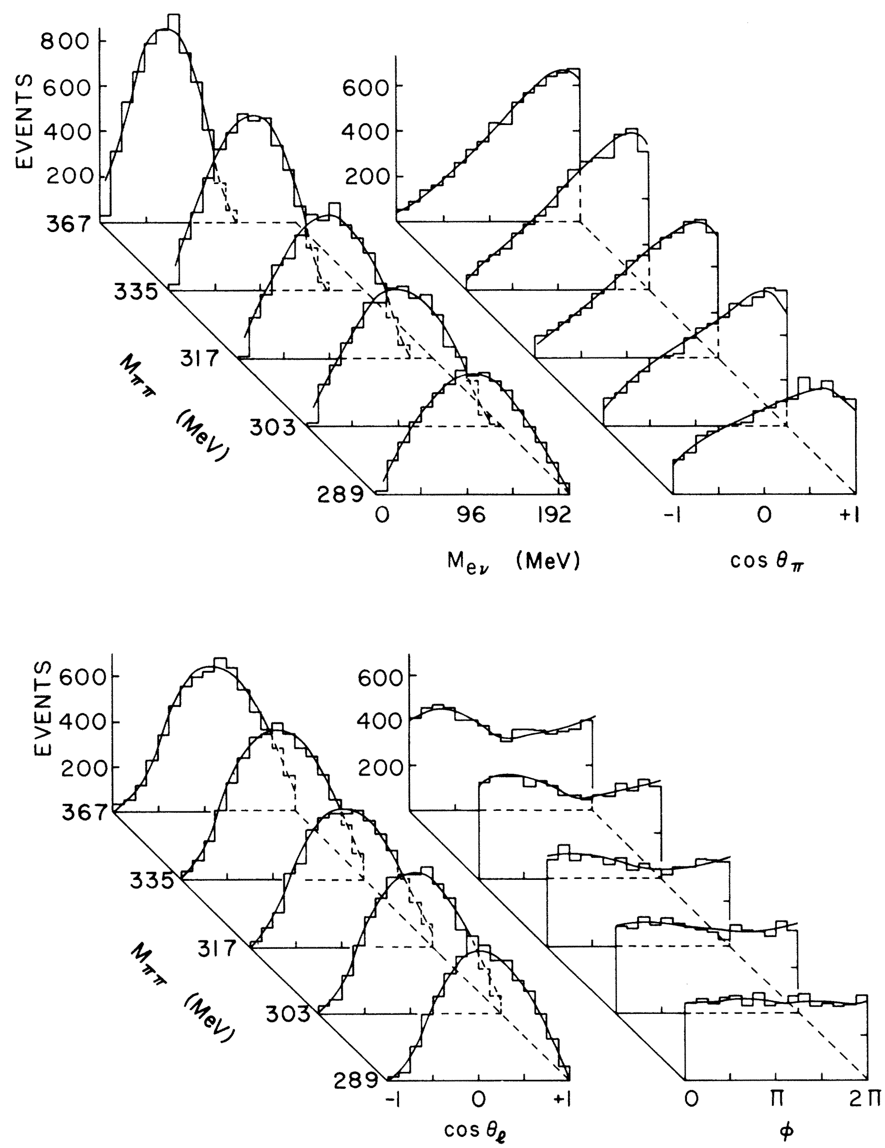

FIG. 11. Projected distributions of the K_{e4} experimental sample on the configuration variables. The curves represent the overall fit.

V. CONCLUSION

This experiment provides an answer to most of the questions which have been raised about K_{e4} decay. In particular, our results help to understand the behavior of the s-wave $\pi\pi$ phase shift at low energy. Once more, we would like to emphasize that the five points obtained for the phase difference $\delta_0^0 - \delta_1^1$ are practically model-independent, whereas the scattering length itself could change, given some refinements in the models or in the analysis of π-production data above 500 MeV. It is also interesting to point out that the above error on a_0^0 contains two contributions, an experimental and a theoretical one, which are almost of the same size. This means that the precision achieved in this experiment compares with the overall accuracy of the present description of low energy $\pi\pi$ interaction.

ACKNOWLEDGMENTS

We are indebted to the CERN staffs of the proton synchrotron and of the computing center for their continuous support throughout the experiment. We deeply acknowledge the excellent work of our technical teams, especially of S. Brehin, R. Ferlicot, G. Tarte, and J.-P. Vittet. We should like also to acknowledge the participation of Dr. L. Sulak in the early part of the experiment and to thank Dr. J. L. Basdevant and Dr. J. L. Petersen for many helpful discussions.

---

*Work supported in part by the Swiss National Fund for Scientific Research and by the French "Commissariat ã l'Energie Atomique."

†Present address: CERN, Geneva, Switzerland.

‡Present address: Department of Physics, University of Wisconsin, Madison, Wisconsin 53706.

[1]S. Weinberg, Phys. Rev. Lett. 17, 336 (1966); 18, 1178(E) (1967).

[2]S. Weinberg, Phys. Rev. Lett. 17, 616 (1966).

[3]P. Bloch *et al.*, Phys. Lett. 60B, 393 (1976).

[4]R. P. Ely *et al.*, Phys. Rev. 180, 1319 (1969); W. Schweinberger *et al.*, Phys. Lett. 36B, 246 (1971).

[5]M. Bourquin *et al.*, Phys. Lett. 36B, 615 (1971); P. Basile *et al.*, *ibid.* 36B, 619 (1971); A. Zylbersztejn *et al.*, *ibid.* 38B, 457 (1972).

[6]E. W. Beier *et al.*, Phys. Rev. Lett. 29, 511 (1972); E. W. Beier *et al.*, *ibid.* 30, 399 (1973).

[7]A. M. Diamant-Berger, Ph.D. thesis, University of Paris, Orsay, 1976 (unpublished).

[8]L. Rosselet, Ph.D. thesis, University of Geneva, 1976 (unpublished).

[9]Beam $m13$. See M. Ferro-Luzzi *et al.*, Report No. CERN NP INT. 73-18 (unpublished).

[10]R. Sachot, Ph.D. thesis, University of Geneva, 1975 (unpublished).

[11]B. Devaux, Thesis, University of Paris, Orsay, 1975 (unpublished); B. Devaux *et al.* (unpublished).

[12]P. Bloch *et al.*, Phys. Lett. 56B, 201 (1975).

[13]A. M. Diamant-Berger *et al.*, Phys. Lett. 62B, 485 (1976).

[14]Particle Data Group, Rev. Mod. Phys. 48, S1 (1976).

[15]N. Cabibbo and A. Maksymowicz, Phys. Rev. 137, B438 (1965); 168, 1926(E) (1968).

[16]A. Pais and S. B. Treiman, Phys. Rev. 168, 1858 (1968).

[17]Our functions α, β, and γ are different from the ones used in Ref. 16.

[18]A. Zylbersztejn, Ph.D. thesis, University of Paris, Orsay, 1972 (unpublished).

[19]P. Basile, J. de Phys. (Paris) 32, C3-45 (1971).

[20]E. Ginsberg, Phys. Rev. 142, 1035 (1966); 162, 1570 (1967); 171, 1675 (1968); Phys. Rev. D 1, 229 (1970).

[21]D. Morgan and M. R. Pennington, Phys. Rev. D 12, 1283 (1975).

[22]L. M. Chounet, J. M. Gaillard, and M. K. Gaillard, Phys. Rep. 4C, 199 (1972).

[23]S. N. Biswas *et al.*, Ann. Phys. (N.Y.) 52, 366 (1969); A. Q. Sarker, Phys. Rev. 176, 1959 (1968); S. N. Biswas *et al.*, Phys. Rev. D 1, 1445 (1970).

[24]J. L. Basdevant, C. D. Froggatt, and J. L. Petersen, Nucl. Phys. B72, 413 (1974).

[25]W. Maenner, in *Experimental Meson Spectroscopy—1974*, proceedings of the Boston Conference, edited by D. A. Garelick (A.I.P., New York, 1974).

[26]V. Shrinivasan *et al.*, Phys. Rev. D 12, 681 (1975).

[27]P. Estabrooks and A. D. Martin, Nucl. Phys. B79, 301 (1974); E. Grayer *et al.*, Nucl. Phys. B75, 189 (1974).

[28]M. David *et al.* (unpublished); G. Villet *et al.* (unpublished).

[29]B. Bonnier and N. Johanneson, Nuovo Cimento 29A, 565 (1975).

[30]J. Franklin, Phys. Rev. D 11, 513 (1975).